Int. J. Solids Structures, 1975, Vol. 11, pp. 33–51. Pergamon Press. Printed in Gt. Britain.

TRANSIENT RESPONSE OF AN ELASTIC PLATE TO LOADS WITH FINITE CHARACTERISTIC DIMENSIONS†

FREDERICK R. NORWOOD‡
Code Application Division, Sandia Laboratories, Albuquerque, New Mexico 87115, U.S.A.

(*Received* 31 *December* 1973; *revised* 15 *April* 1974)

Abstract—The present paper uses a recently developed technique to obtain solutions for an elastic plate acted upon by loads with finite characteristic dimensions. Exact two dimensional transform solutions are derived for a plate suddenly loaded on one of its bounding surfaces. The transform solutions for a general load are rearranged into infinite sums representing multiply-reflected shear and dilatational waves. The interpretation of the infinite sums is verified by ray tracing. The final expressions are used to deduce the Green's function for the velocity. Numerical results are presented for a step function input.

INTRODUCTION

In recent years, several computer codes have been developed to solve wave propagation problems for linear and non-linear material laws. These codes involve loads applied over finite spatial regions. The development of the codes was made necessary by the practical application of the solutions to determining structural response, and also by the fact that the analytical solution of problems involving these loads leads to extremely difficult mathematical analyses, even with simple linear material laws. Although the numerical codes have been used to solve very complicated, but realistic problems, there remain many questions as to their accuracy. Within this context, the present work, dealing with an elastic plate, is intended as a sample solution for comparing computer generated solutions.

The most common elastic sources that have been used in the past are points, infinite lines, and plane sources. However, very few analytical papers dealing with finite loads have been published, and much work is needed in this area. The simplest problem in this category is that of an axially symmetric load, and, for this case, solutions exist for various material geometries [1–5]. To consider more general types of sources, the author undertook the task of developing analytical tools to solve problems with finite sources [6–8]. The key to the development was the introduction of a parameter which acted as the spatial analog of artificial viscosity. The parameter made possible an extension of de Hoop's transformation to problems where the solution has singularities on the real axis of the Fourier transform plane. The present paper contains the necessary analysis for finite loads on a plate.

In references [6–8], there was only one "interface," and no reflected or transmitted waves appeared. Results will now be obtained for two or more interfaces. These results will be derived by the technique of reflectivity and transmissibility coefficients. The technique

† This research was supported by the United States Atomic Energy Commission.
‡ Member of Technical Staff, Code Application Division.

consists of finding the n-th reflected and transmitted waves from the $(n-1)$-th reflected and transmitted waves. To consider types of problems more general than those treated previously, one must begin by developing suitable reflectivity and transmissibility coefficients for various kinds of interface conditions. The reflectivity coefficients to be presented here are intended to serve as a guide for developing three dimensional reflectivity and transmissibility coefficients, and are most closely related to those discussed by Phinney[9]. These coefficients relate the displacement potentials of the incoming field to the displacement potentials of the reflected field.

An elastic plate is the simplest structure where interfaces become important. In fact, in many respects, wave propagation in elastic plates is analogous to propagation in layered spaces, as was indicated in [26, p. 281]. Procedures for developing solutions can be very similar, and several wave types encountered in layered-space problems also appear in plate problems. By these arguments, it seems reasonable to investigate wave propagation in a plate and develop requisite reflectivity and transmissibility coefficients. The problem of a plate suddenly impacted on one of its bounding surfaces is considered here, and the exact two dimensional transform solution is derived for general loading conditions. The transform solution is then rearranged into infinite sums representing multiply reflected shear and dilatational waves. The interpretation of the infinite sums is verified by doing a ray tracing analysis of the problem. This ray tracing involves the use of reflectivity coefficients which are derived in the process. As in [6], the present two dimensional work will serve as the basis for the forthcoming three dimensional analysis.

The general results are used to find the Green's function for the velocity. This Green's function is then used to deduce numerical results for a step function stress input over half of a bounding surface.

PLANE CASE

The basic ideas will be developed via the two-dimensional case. These ideas will be presented in detail since they are directly applicable to the three-dimensional case. The reader is assumed to be familiar with Cagniard's technique as given in [6–8]. After the posing of the problem, the formal solution will be obtained by the usual application of integral transforms. Ray theory will then be used to rederive the formal solution. Ray theory will be the main tool for solving the three dimensional plate problem and layered half space problems with finite loads.

Statement of the problem

In a rectangular coordinate system, consider an elastic plate confined to $0 \leq y \leq h$. A normal load is suddenly applied, at time $t = 0$, to the surface $y = 0$, as shown in Fig. 1. The governing wave equations are

$$c_1^2 \nabla^2 \Phi = \frac{\partial^2 \Phi}{\partial t^2}, \; c_2^2 \nabla^2 \psi = \frac{\partial^2 \psi}{\partial t^2}, \qquad \nabla \cdot \psi = 0. \tag{1}$$

The potentials Φ and ψ are related to the displacements through

$$\mathbf{u} = \nabla \Phi + \nabla x \psi, \tag{2}$$

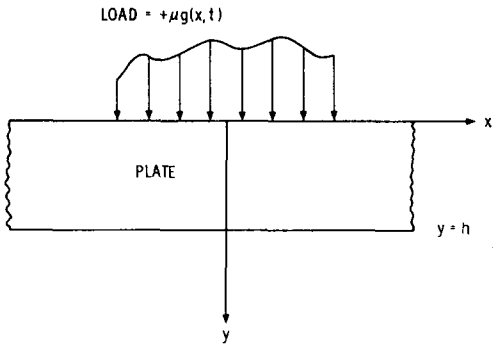

Fig. 1. Geometry of the general problem.

where c_1 and c_2 are the wave speeds, $\rho c_1^2 = \lambda + 2\mu$, $\rho c_2^2 = \mu$, λ and μ are the Lamé constants, and ρ is the material density. The stress–strain relations needed in the sequel are

$$\tau_{ij} = \lambda \nabla^2 \Phi \delta_{ij} + 2\mu \varepsilon_{ij}, \qquad \varepsilon_{ij} = \frac{1}{2}\left(\frac{\partial u_i}{\partial x_j} + \frac{\partial u_j}{\partial x_i}\right), \tag{3}$$

where δ_{ij} is the Kronecker delta. The initial conditions are taken as

$$\Phi(x, y, 0) = \partial\Phi(x, y, 0)/\partial t = \psi(x, y, 0) = \partial\psi(x, y, 0)/\partial t = 0,$$

representing quiescence at $t = 0$. It will be assumed† that u_z vanishes everywhere and that u_x and u_y are independent of z. These assumptions give $\tau_{yz} = \tau_{xz} = \varepsilon_{zz} = 0$, and $\boldsymbol{\psi} = \psi \mathbf{e}_z$, where $\mathbf{e}_z$ is the unit vector in the z direction. The boundary conditions for the problem are

$$\tau_{xy}(x, h, t) = \tau_{yy}(x, h, t) = \tau_{xy}(x, 0, t) = 0, \tag{4}$$

$$\tau_{yy}(x, 0, t) = \mu g(x, t), \tag{5}$$

where $g(x, t)$ is the loading function.

Formal solution

The one-sided and two-sided Laplace transforms to be used here are defined, respectively, by the equations

$$\tilde{f}(x, y, p) = L(f) = \int_0^\infty f(x, y, t) e^{-pt}\, dt, \tag{6a}$$

$$f(x, y, t) = \frac{1}{2\pi i}\int_{c-i\infty}^{c+i\infty} \tilde{f}(x, y, p) e^{pt}\, dp, \tag{6b}$$

$$\tilde{f}^L(k, y, p) = \int_{-\infty}^{\infty} \tilde{f}(x, y, p) e^{pkx}\, dx, \tag{7a}$$

$$\tilde{f}(x, y, p) = \frac{p}{2\pi i}\int_{-i\infty-\varepsilon}^{i\infty-\varepsilon} \tilde{f}^L(k, y, p) e^{-pkx}\, dk, \tag{7b}$$

where c is chosen to the right of any singularity of $\tilde{f}$. In accordance with Lerch's theorem

† These assumptions yield the plane strain case[10, p. 11].

[11, p. 345], it is sufficient to assume in (7) that p is a real positive number, for this guarantees a unique inverse. In (7b) the path of integration lies within the strip of convergence [12].

The application of (6a and 7a) to the first of equations (1), using the indicated initial conditions, leads to the ordinary differential equation for $\tilde{\Phi}^L$ and its solution

$$\frac{d^2\tilde{\Phi}^L}{dy^2} + p^2k^2\tilde{\Phi}^L = a_1{}^2p^2\tilde{\Phi}^L, \qquad a_ic_i = 1, \tag{8}$$

$$\tilde{\Phi}^L(k, y, p) = A(k, p)e^{-p\eta_1(k)y} + B(k, p)e^{p\eta_1(k)y} \tag{9}$$

$$\eta_i(k) = (a_i{}^2 - k^2)^{1/2}, \; Re\eta_i(k) > 0, \tag{10}$$

where for definiteness the branch $Re\eta_i > 0$ is selected. Similarly, one finds that

$$\tilde{\psi}^L(k, y, p) = C(k, p)e^{-p\eta_2(k)y} + D(k, p)e^{p\eta_2(k)y}. \tag{11}$$

The transform of the stress equations (3) leads to

$$\begin{aligned}\tilde{\tau}^L_{yy}(k, y, p)/\mu p^2 = {} & (a_2{}^2 - 2k^2)\tilde{\Phi}^L(k, y, p) + 2k\eta_2(k)[-C(k, p)e^{-p\eta_2(k)y} \\ & + D(k, p)e^{p\eta_2(k)y}],\end{aligned} \tag{12}$$

$$\begin{aligned}\tilde{\tau}^L_{yy}(k, y, p)/\mu p^2 = {} & (a_2{}^2 - 2k^2)\tilde{\psi}^L(k, y, p) - 2k\eta_1(k)[-A(k, p)e^{-p\eta_1(k)y} \\ & + B(k, p)e^{p\eta_1(k)y})].\end{aligned} \tag{13}$$

The application of the boundary conditions (4 and 5) yields, after some algebra,

$$\begin{aligned}\frac{2p^2(a_2{}^2 - 2k^2)A(k, p)}{\tilde{g}^L(k, p)} = {} & \mathcal{M}(k, X, Y)[R^2(k)(1 - XY) + S^2(k)Y(X - Y) \\ & + R(k)S(k)(1 - Y^2)],\end{aligned} \tag{14}$$

$$\begin{aligned}\frac{2p^2(a_2{}^2 - 2k^2)B(k, p)}{\tilde{g}^L(k, p)} = {} & \mathcal{M}(k, X, Y)[R^2(k)XY(XY - 1) - S^2(k)X(X - Y) \\ & + R(k)S(k)X^2(Y^2 - 1)],\end{aligned} \tag{15}$$

$$\frac{p^2C(k, p)}{2k\eta_1(k)\tilde{g}^L(k, p)} = \mathcal{M}(k, X, Y)[R(k)(XY - 1) - S(k)X(X - Y)], \tag{16}$$

$$\frac{p^2D(k, p)}{2k\eta_1(k)\tilde{g}^L(k, p)} = \mathcal{M}(k, X, Y)[R(k)XY(XY - 1) - S(k)Y(X - Y)]. \tag{17}$$

In these expressions, one defines

$$\begin{aligned}&R(k) = (a_2{}^2 - 2k^2)^2 + 4k^2\eta_1(k)\eta_2(k), \\ &S(k) = (a_2{}^2 - 2k^2)^2 - 4k^2\eta_1(k)\eta_2(k), \\ &X = \exp[-p\eta_1(k)h], \qquad Y = \exp[-p\eta_2(k)h], \\ &1/\mathcal{M}(k, X, Y) = R^2(k)(XY - 1)^2 - S^2(k)(X - Y)^2;\end{aligned}$$

$\tilde{g}^L(k, p)$ and $R(k)$ are identified, respectively, as the double transform of $g(x, t)$ and the the Rayleigh characteristic function.

The solution to the plate problem may be obtained in a wave expansion form by the technique of Article 41, Reference [13]. The technique has been used in [1, 2, 14–22]. The convergence of the resulting series has been discussed by Mencher[21] for a three-dimensional point source, who also outlines the next steps to be taken in the solution. The wave expansion

form may be obtained by writing $\mathscr{M}(k, X, Y)$ as

$$1/\mathscr{M}(k, X, Y) = R^2(k)[1 - 2XY + X^2Y^2 - S^2(k)(X - Y)^2/R^2(k)], \tag{18}$$

and expanding in the neighborhood of $(X = 0,\ Y = 0)$. This can be done by a Taylor series expansion[1] or by using the relation $1/(1 - z) = \sum_0^\infty z^n$ valid for $|z| < 1$ [2 and 14–21]. This gives the infinite sum $\mathscr{S}$ defined by†

$$\left.\begin{aligned} \mathscr{S} = R^2(k)\mathscr{M}(k, X, Y) &= \sum_{n=0}^{\infty} (\alpha + \beta)^n, \\ \alpha = 2XY + M^2(k)(X - Y)^2, &\qquad \beta = -X^2Y^2,\ M(k) = S(k)/R(k). \end{aligned}\right\} \tag{19}$$

Equations (14–17) may now be written in the desired wave expansion form:

$$p^2A(k, p)R^2(k) = \tilde{g}^L(k, p)(a_2{}^2 - 2k^2)\{R(k) + [S(k) - R(k)]XY - S(k)Y^2\}\mathscr{S}, \tag{20}$$

$$p^2C(k, p)R^2(k) = 2k\eta_1(k)\tilde{g}^L(k, p)\{-R(k) + [R(k) + S(k)]XY - S(k)X^2\}\mathscr{S}, \tag{21}$$

$$2R^2(k)p^2(a^2 - 2k^2)B(k, p) = \tilde{g}^L(k, p)\{[S^2(k) - R^2(k)]XY - S(k)[S(k) + R(k)]X^2 + R(k)[R(k) + S(k)]X^2Y^2\}\mathscr{S}, \tag{22}$$

$$p^2D(k, p)R^2(k) = 2k\eta_1(k)\tilde{g}^L(k, p)\{-[R(k) + S(k)]XY + S(k)Y^2 + R(k)X^2Y^2\}\mathscr{S}. \tag{23}$$

The substitution of (20–23) leads to the analog of equation (24) in Ref. [21], where it was stated that the resulting form "strongly suggests that each integral (resulting from the infinite sums) is the mathematical representation of one of the reflected waves." The same interpretation is given in [14–22]. In the next section, it will be shown that this interpretation is correct, provided that like powers of X^2, XY, and Y^2 be grouped together.

The usual application of transform calculus had led, after considerable algebra, to equations (20–23). In most applications, however, one is interested only in a few reflections; thus, most of the terms in these equations provide superfluous information. The ray tracing technique of the next section will provide the terms required for the first few reflections in a more straightforward manner.

Ray tracing solution

The solution to the posed problem may be obtained in a wave expansion form by considering three canonical problems. These canonical problems generate reflectivity coefficients that may be used in other problems. Figure 2 presents the geometry of these problems.

Canonical problem A

For this problem, one considers an elastic half-plane to which a normal load is suddenly applied, at time $t = 0$, at the surface $y = 0$. Equations (1–5) are applicable here, with (4) replaced by the single condition

$$\tau_{xy}(x, 0, t) = 0. \tag{24}$$

The solution for the half plane are obtained by setting $B(k, p)$ and $D(k, p)$ in equations (9–13) equal to zero, and deleting the boundary conditions at $y = h$. In this case, one finds

$$p^2A(k, p)R(k) = \tilde{g}^L(k, p)(a_2{}^2 - 2k^2), \tag{25}$$

$$p^2C(k, p)R(k) = -2k\eta_1(k)\tilde{g}^L(k, p). \tag{26}$$

† This step will be justified by the ray tracing solution.

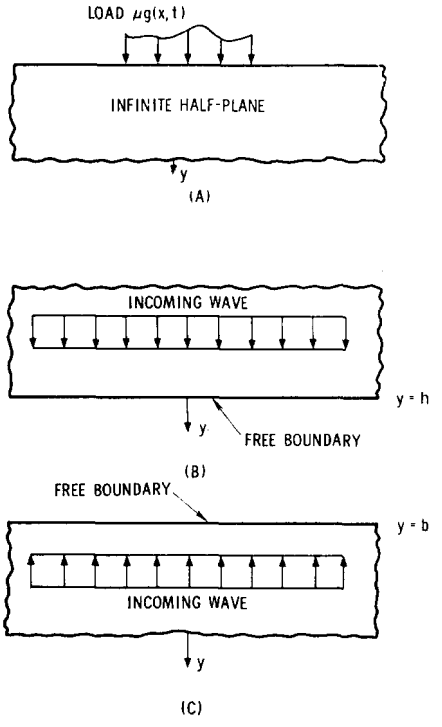

Fig. 2. Geometry for the canonical problems A, B and C.

These two expressions represent the limit of equations (20–23) as either p or h approach infinity. The limit $p \to \infty$ yields the short time solution which is valid for $t < a_1 h$, where $a_1 h$ represents the dilatational travel time to the surface $y = h$. The limit $h \to \infty$ converts the plate into a half-plane. These two limits are obtained from equations (20–23) by setting $X = Y = 0$, to obtain $B(k, p) = D(k, p) = 0$ and also equations (25 and 26).

Canonical problem B

In this problem, a half-plane is given by $y < h$, with the free boundary at $y = h$. The incident wave is given by the potentials

$$\tilde{\Phi}_p^L(k, y, p) = A(k, p)_i e^{-p\eta_1(k)y}, \tag{27}$$

$$\tilde{\psi}_p^L(k, y, p) = C(k, p)_i e^{-p\eta_2(k)y}. \tag{28}$$

where the subscript p indicates the direction of the incident wave (positive y-direction). In this problem one needs to determine the potentials of the reflected field using the stress boundary conditions at the surface $y = h$. The reflected potentials are given by

$$\tilde{\Phi}_r^L(k, y, p) = B(k, p)_r e^{p\eta_1(k)y}, \tag{29}$$

$$\tilde{\psi}_r^L(k, y, p) = D(k, p)_r e^{p\eta_2(k)y}. \tag{30}$$

The total field is the sum of the incoming and reflected field, and is given by equations (9–13), with the proper subscripts added. The application of the boundary conditions

leads to

$$R(k)D(k,p)_r = -4k\eta_1(k)(a_2{}^2 - 2k^2)XYA(k,p)_i - S(k)Y^2C(k,p)_i, \tag{31}$$

$$R(k)B(k,p)_r = 4k\eta_2(k)(a_2{}^2 - 2k^2)XYC(k,p)_i - S(k)X^2A(k,p)_i. \tag{32}$$

To identify the reflectivity coefficients, one now writes (29 and 30) in the form

$$\begin{pmatrix}\tilde{\Phi}_r{}^L(k,y,p)\\ \tilde{\psi}_r{}^L(k,y,p)\end{pmatrix} = \mathscr{H}(y-h)\mathscr{R}_P\begin{pmatrix}\tilde{\Phi}_P{}^L(k,h,p)\\ \tilde{\psi}_P{}^L(k,h,p)\end{pmatrix}, \tag{33}$$

$$\mathscr{H}(y-h) = \begin{pmatrix}e^{p\eta_1(k)(y-h)} & 0\\ 0 & e^{p\eta_2(k)(y-h)}\end{pmatrix}, \tag{34}$$

$$\mathscr{R}_P = \begin{pmatrix}R_{DDP} & R_{SDP}\\ R_{DSP} & R_{SSP}\end{pmatrix}, \tag{35}$$

$$R_{DDP} = -M(k) = R_{SSP}$$
$$R_{SDP} = 4k\eta_2(k)(a_2{}^2 - 2k^2)/R(k),$$
$$R_{DSP} = -\eta_1(k)R_{SDP}/\eta_2(k),$$

where the first subscript in the reflectivity coefficients indicates the kind of incoming wave (shear or dilatation); the second subscript, the kind of reflected wave; and the third subscript, the direction of the incident wave.

Canonical problem C

In this problem, a half space is given by $y > b$, with the free boundary at $y = b$. The incident wave is given in terms of the elastic potentials and one must find the potentials of the reflected wave. The potentials for the problem are obtained from equations (27–32) by interchanging the subscripts i and r, and by setting $h = b$, $P = N$. This leads to

$$\begin{pmatrix}\tilde{\Phi}_r{}^L(k,y,p)\\ \tilde{\psi}_r{}^L(k,y,p)\end{pmatrix} = \mathscr{H}(b-y)\mathscr{R}_N\begin{pmatrix}\tilde{\Phi}_N{}^L(k,b,p)\\ \tilde{\psi}_N{}^L(k,b,p)\end{pmatrix}, \tag{36}$$

$$\mathscr{R}_N = \begin{pmatrix}R_{DDN} & R_{SDN}\\ R_{DSN} & R_{SSN}\end{pmatrix} = \mathscr{R}_P{}^{-1}, \tag{37}$$

$$R_{DDN} = -M(k) = R_{SSN},$$
$$R_{SDN} = -4k\eta_2(k)(a_2{}^2 - 2k^2)/R(k),$$
$$R_{DSN} = -\eta_1(k)R_{SDN}/\eta_2(k).$$

Application of the results

In the original formulation of the problem, there were 4 unknowns which were found from equations (12 and 13) by applying the boundary conditions. Each of the canonical problems A, B and C involved only two unknowns. Thus, in each case, the algebra involved was simpler than for the original problem. The results of these problems will now be used to generate the displacement potentials of the original problem

Define these potentials as the infinite sum

$$\begin{pmatrix}\tilde{\Phi}^L(k,y,p)\\ \tilde{\psi}^L(k,y,p)\end{pmatrix} = \sum_{n=1}^{\infty}\begin{pmatrix}\tilde{\Phi}^L(k,y,p)\\ \tilde{\psi}^L(k,y,p)\end{pmatrix}_n. \tag{38}$$

where the first term is obtained directly from the canonical problem A and the subsequent terms are found recursively as will be indicated. From the results of problem A

$$\begin{pmatrix}\tilde{\Phi}^L(k, y, p)\\ \tilde{\psi}^L(k, y, p)\end{pmatrix}_1 = G(k, p)\mathscr{H}(-y)\mathscr{A}(k) \tag{39}$$

$$\mathscr{A} = \begin{pmatrix}a_2{}^2 - 2k^2\\ -2k\eta_1(k)\end{pmatrix}, \quad G(k, p) = \tilde{g}^L(k, p)/p^2 R(k). \tag{40}$$

The first solution is now used as the incident wave for the canonical problem B, and the results represent the second term of the sum. Thus

$$\begin{pmatrix}\tilde{\Phi}^L(k, y, p)\\ \tilde{\psi}^L(k, y, p)\end{pmatrix}_2 = G(k, p)\,\mathscr{H}(y - h)\mathscr{R}_P\,\mathscr{H}(-h)\mathscr{A}(k). \tag{41}$$

This now serves as the incident wave for the canonical problem C, where b is selected as zero, and the resulting expression corresponds to the third term of the sum; that is,

$$\begin{pmatrix}\tilde{\Phi}^L(k, y, p)\\ \tilde{\psi}^L(k, y, p)\end{pmatrix}_3 = G(k, p)\mathscr{H}(-y)\mathscr{R}_N\,\mathscr{H}(-h)\mathscr{R}_p\,\mathscr{H}(-h)\mathscr{A}(k). \tag{42}$$

The process is now repeated whereby the expression for the $(2n-1)$-th term serves as the incident wave for the canonical problem B, thereby producing the $2n$-th term. Then the $2n$-th term serves as the incident wave for the canonical problem C, thereby producing the $(2n+1)$-th term. By this recursive process, one finds that

$$\begin{pmatrix}\tilde{\Phi}^L(k, y, p)\\ \tilde{\psi}^L(k, y, p)\end{pmatrix}_{2n+1} = G(k, p)\,\mathscr{H}(-y)\mathscr{M}^n\mathscr{A}(k), \qquad n = 0, 1, 2, \ldots, \tag{43}$$

$$\begin{pmatrix}\tilde{\Phi}^L(k, y, p)\\ \tilde{\psi}^L(k, y, p)\end{pmatrix}_{2n+2} = G(k, p)\,\mathscr{H}(y - h)\mathscr{R}_p\,\mathscr{H}(-h)\,\mathscr{M}^n\mathscr{A}(k), \qquad n = 0, 1, 2, \ldots, \tag{44}$$

where $\mathscr{M}$ represents the matrix for a reflection at each surface; that is, $\mathscr{M} = \mathscr{R}_N\mathscr{H}(-h)\cdot \mathscr{R}_p\mathscr{H}(-h)$. This reduces to

$$\mathscr{M} = \begin{pmatrix}m_{11}, & m_{12}\\ m_{21}, & m_{22}\end{pmatrix}, \tag{45}$$

$$\begin{aligned} m_{11} &= X[R_{DDN}^2 X - R_{SDN} R_{DSN} Y],\\ m_{12} &= Y R_{DDN} R_{SDN}(Y - X),\\ m_{21} &= X R_{DDN} R_{DSN}(X - Y),\\ m_{22} &= Y[R_{DDN}^2 Y - R_{DSN} R_{SDN} X],\\ R_{SDN} R_{DSN} &= M^2(k) - 1. \end{aligned}$$

This matrix satisfies the characteristic equation

$$\mathscr{M}^2 = \alpha\mathscr{M} + \beta I, \tag{46}$$

where α and β are given by equation (19). This equation may be used recursively to find powers of $\mathscr{M}$ in terms of $\mathscr{M}$ and the identity matrix I. This gives†

† Recall that $[n/2] = n/2$ if n is even, and $[n/2] = (n-1)/2$ if n is odd. These results were obtained by the recursive scheme shown in Appendix A.

$$\mathscr{M}^n = a_n\mathscr{M} + b_n I, \qquad a_1 = 1, b_1 = 0, \tag{47}$$

$$a_{n+1} = \sum_{r=0}^{[n|2]} \binom{n-r}{r} \alpha^{n-2r}\beta^r, \qquad n = 0, 1, 2, \ldots, \tag{48}$$

$$b_{n+2} = \beta a_{n+1}, \qquad n = 0, 1, 2, \ldots. \tag{49}$$

Expression (38), with the auxiliary relations (39–49) represents a rearrangement of equations (20–23) such that equal power of X^2, XY and Y^2 are grouped together. This may be seen more easily by writing

$$\begin{pmatrix} \tilde{\Phi}^L(k, y, p) \\ \tilde{\psi}^L(k, y, p) \end{pmatrix} = G(k, p)[\mathscr{H}(-y) + \mathscr{H}(y-h)\mathscr{R}_p\mathscr{H}(-h)] \sum_{n=0}^{\infty} \mathscr{M}^n\mathscr{A}(k). \tag{50}$$

The term $n = 0$ generates the lowest order terms in powers of X^2, Y^2, and XY in equations (20–23). The term $n = 1$ gives the second lowest terms in equations (20–23), and so on. Thus, in equation (50), the term $n = 0$ represents the waves arising from the impact loading and the first reflection, and the nth term represents the waves arising from the $(n-1)$-th reflection at the surface $y = 0$ and the nth reflection at the surface $y = h$. Equation (50) contains all the information in equations (20–23).

Having verified that equation (50) reproduces the results of equations (20–23), one now proceeds to writing a_n in a more useful form. This is done by using the explicit values of α and β given by (19). The desired form is†

$$a_n = \sum_{r=0}^{n-1} \binom{n+r}{n-1-r} (XY)^{n-1-r} D^r, \qquad n = 1, 2, 3 \ldots,$$
$$D = M^2(k)(X - Y)^2.$$

Discussion of the plane case

The plane case has served to verify in detail the equivalence of the formal transform solution and the ray tracing solution. This is an important verification which gives validity to the previous papers where such an equivalence was assumed. The ray tracing method conveniently separates like power of X^2, XY and Y^2, corresponding to separating the waves in order of reflection. Thus, for a given value of t, one may easily decide how many terms are needed in the solution. The form of the solution as given by equations (43 and 44) seems to be the best suited for applications.

The details for the plane case have been presented here primarily for the reason that the procedure will be applicable to more complicated problems. For these problems, the ray tracing details need not be repeated, but those details peculiar to the more complicated problems may then be included in the analysis. For example, in the three dimensional case, one may abbreviate the details connected with equations (38–45), and proceed to write equations corresponding to equations (46–50).

Sample problem

To effect the final inversion, $\tilde{g}^L(k, p)$ must first be specified. Suppose, as an example, that $g(x, t)\mu$ is a uniform load applied for $x > 0$, and, to determine the Green's function in time, suppose that $g(x, t)$ has a Dirac delta function behavior in time:

$$g(x, t) = -\delta(t)H(x). \tag{51}$$

† See Appendix A.

As was done in[6–8], this loading function is considered as the limit $\xi \to 0$ of the expression $[-\exp(-x\xi)\delta(t)H(x)]$, where the limit will be taken at an appropriate step in the solution. The formal application of the transforms to this bracketted expression gives

$$\tilde{g}^L(k, p) = \frac{1}{pk - \xi}, \qquad -\infty < \mathscr{R}ek < \xi/p, \tag{52}$$

with the indicated strip of convergence. This means that ε in equation (7b) may be selected as zero. To illustrate the form of the contributions, one now proceeds to find the velocity in the interior of the plate.

From equation (2), it follows that

$$\tilde{v}_x{}^L(k, y, p) = -p^2 \sum_{n=1}^{\infty} [k\tilde{\Phi}^L(k, y, p)_n - \eta_2(k)(-1)^n \tilde{\psi}^L(k, y, p)_n], \tag{53}$$

$$\tilde{v}_y{}^L(k, y, p) = p^2 \sum_{n=1}^{\infty} [k\tilde{\psi}^L(k, y, p)_n + \eta_1(k)(-1)^n \tilde{\Phi}^L(k, y, p)_n]. \tag{54}$$

The details of the inversion of the two-sided Laplace transform on x are similar to those in [23], and therefore only an outline of these details will be given here. From equations (47, 50 and 52), it follows that there are three cases to be outlined below that need to be investigated. In each case, the singularities in the k-plane of the integrand are the branch points at $\pm a_1$, $\pm a_2$, and the simple poles at $\pm 1/c_R$, and ξ/p, where c_R is the Rayleigh speed (Fig. 3). From the results of [6 and 23], one concludes that the solution will have the form

$$v_j(x, y, t) = v_{1j}(x, y, t) + v_{2j}(x, y, t), \qquad j = x, y,$$

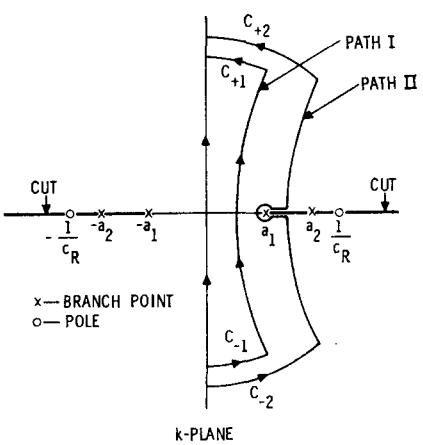

Fig. 3. Integration paths in the k-plane.

for $x > 0$, where v_{1j} represents plane waves directly under the load, and v_{2j} represents the remainder of the velocity. For $x < 0$, one obtains equations analogous to (27 and 28) of [6]; that is

$$v_{2x}(x, y, t) = v_{2x}(-x, y, t),$$
$$v_{2y}(x, y, t) = -v_{2y}(-x, y, t).$$

Therefore, it is sufficient to direct attention to the region $x > 0$.

The first case involves terms of the form

$$\tilde{f}_1^{\,L}(k, y, p) = \frac{F_1(k)}{pk - \xi} \exp[-p\eta_1(k)z], \tag{55}$$

where z is a function of y, h, and n. This form leads to the inversion integral

$$\tilde{f}_1(x, y, p) = \frac{p}{2\pi i}\int_{-i\infty}^{i\infty} \frac{F_1(k)}{pk - \xi} \exp[-p\eta_1(k)z - pkx]\, \mathrm{d}k. \tag{56}$$

As was done in[23], for $x > 0$ one closes the contour to the right of the integration path, as shown in Fig. 3. Paths I and II are Cagniard paths [25] along which $Im(\eta_i z + kx) = 0$, $i = 1, 2$. This results in

$$\tilde{f}_1(x, y, p) = -F_1(\xi/p)\exp[-p\eta_1(\xi/p)z - x\xi] + \frac{p}{2\pi i}\int_{\text{Path I}} \frac{F_1(k)}{pk - \xi} \exp[-p\eta_1(k)z - pkx]\, \mathrm{d}k. \tag{57}$$

It is now appropriate to take the limit as ξ goes to zero. Then, the first term is identified as the Laplace transform of $-F_1(0)\delta(t - a_1 z)$, and the second term is transformed as in equation (18), Ref.[23]. The final result for this case is

$$f_1(x, y, t) = -F_1(0)\delta(t - a_1 z) + \mathscr{R}e\left[\frac{F_1(k_1)}{k_1 \pi i}\frac{\partial k_1}{\partial t}\right]\chi_1(t, x, z) \tag{58}$$

$$\chi_1(t, x, z) = H(t - a_1\rho), \qquad \rho^2 = x^2 + z^2$$

$$k_1(x, z, t) = \frac{xt}{\rho^2} + \frac{iz(t^2 - a_1{}^2\rho^2)^{1/2}}{\rho^2},$$

and k_1 was deduced from $t - k_1 x - \eta_1(k_1)z = 0$. Terms of the form (55) represent waves which started as dilatation and their dilatational reflections.

For the second case, one has terms of the form

$$\tilde{f}_2^{\,L}(k, y, p) = \frac{F_2(k)}{pk - \xi} \exp[-p\eta_2(k)z]. \tag{59}$$

The inversion integral is

$$\tilde{f}_2(x, y, p) = \frac{p}{2\pi i}\int_{-i\infty}^{i\infty} \frac{F_2(k)}{pk - \xi} \exp[-p\eta_2(k)z - pkx]\, \mathrm{d}k.$$

By closing this contour to the right of the integration path shown in Fig. 3, one finds that

$$\tilde{f}_2(x, y, p) = -F_2(\xi/p)\exp[-p\eta_2(\xi/p)z - x\xi] + \frac{p}{2\pi i}\int_{\text{Path II}} \frac{F_2(k)}{pk - \xi} \exp[-p\eta_2(k)z - pkx]\, \mathrm{d}k.$$

Proceeding as for equation (57), one finds, using also the results of [23],

$$f_2(x, y, t) = -F_2(0)\delta(t - a_2 z) + \mathscr{R}e \sum_{l=2,3} \frac{F_2(k_l)}{k_l \pi i} \frac{\partial k_l}{\partial t} \chi_l(t, x, z) \tag{60}$$

$$\chi_2 = H(t - a_2 \rho),$$

$$x_3 = H[t - a_1 x - z(a_2^2 - a_1^2)^{1/2}] - H(t - a_2 \rho),$$

$$k_2(x, z, t) = \frac{tx}{\rho^2} + \frac{iz}{\rho^2}(t^2 - a_2^2 \rho^2)^{1/2},$$

$$k_3(x, z, t) = \frac{tx}{\rho^2} - \frac{z}{\rho^2}(a_2^2 \rho^2 - t^2)^{1/2},$$

where k_2 and k_3 were deduced from $t - k_l x - \eta_2(k_l)z = 0$. The term $l = 3$ is applicable only for x in the range $c_1 x > c_2 \rho$.

The third case is a generalization of the preceding two cases and involves terms of the form

$$\tilde{f}_3^L(k, y, p) = \frac{F_3(k)}{pk - \xi} \exp[-p\eta_1(k)w - p\eta_2(k)z]. \tag{61}$$

This case reduces to either the first or the second case, depending on whether z or w are identically zero. In this discussion, however, z and w will be assumed nonzero. For $x > 0$, once again, the contour is closed to the right of the integration path. The details of the integration are similar to those in the first case, resulting in

$$\tilde{f}_3(x, y, p) = -F_3(\xi/p)\exp[-p\eta_1(\xi/p)w - p\eta_2(\xi/p)z - x\xi] + \frac{p}{2\pi i} \int_{\text{Path III}} \frac{F_3(k)}{pk - \xi} \exp[-p\eta_1(k)w - p\eta_2(k)z - pkx]\, dk, \tag{62}$$

where Path III is also a Cagniard path along which $Im[\eta_1(k)w + \eta_2(k)z + kx] = 0$. Continuing as for equation (57), one finds the final result for this case:

$$f_3(x, y, t) = -F_3(0)\delta(t - a_1 w - a_2 z) + \mathscr{R}e\left[\frac{F_3(k_4)}{k_4 \pi i} \frac{\partial k_4}{\partial t}\right] \chi_4(t, x, z, w), \tag{63}$$

$$\chi_4(t, x, z, w) = H(t - t_3), \tag{64}$$

where k_4, as a function of x, z, w, and t, is deduced from

$$t - \eta_1(k_4)w - \eta_2(k_4)z - k_4 x = 0, \tag{65}$$

and, like k_1, k_4 has a positive imaginary part. t_3 represents the value of t at the intercept of Path III with the real axis.† Chapter 5 and Appendix I of Ref.[24] discuss various properties of k_4 on the Cagniard path; however, for the present paper, these discussions need to be expanded to cover information needed for a numerical evaluation of the results. For clarity's sake, this expansion will be accomplished in Appendix B. From the results of Appendix B, $t_3 \geq a_1 w + a_2 z$.

† Appendix B indicates how t_3 may be found.

Since all of the difficulties which might be encountered in the transform inversion of $\tilde{v}_x{}^L$ and $\tilde{v}_y{}^L$ have already been treated in equations (55–65), it now remains to determine the specific form of f_1, f_2, and f_3 arising from each value of n in equations (53–54). It seems reasonable to expect that, just as in the case of $\tilde{\Phi}_n$, ψ_n, $\mathscr{M}^n$, and a_n, a general form could be derived for f_i. Rather than to spend some effort deriving this general form, one now proceeds to obtain specific contributions to v_x and v_y. These contributions will be given by $v_i(x, y, t, \Phi_n)$ and $v_i(x, y, t, \psi_n)$, $i = x, y$.

From equation (43),

$$\tilde{\Phi}^L(k, y, p)_1 = \frac{\tilde{g}^L(k, p)}{p^2 R(k)} (a_2{}^2 - 2k^2) e^{-p\eta_1(k)y}, \tag{66}$$

$$\tilde{\psi}^L(k, y, p)_1 = -2k\eta_1(k) \frac{\tilde{g}^L(k, p)}{p^2 R(k)} e^{-p\eta_2(k)y}. \tag{67}$$

This leads to

$$\tilde{v}_x{}^L(k, y, p, \Phi_1) = -\frac{k(a_2{}^2 - 2k^2)}{R(k)(pk - \xi)} e^{-p\eta_1(k)y},$$

which is of the form (55), with $F_1(k) = -k(a_2{}^2 - 2k^2)/R(k)$, and $z = y$. Thus, by equation (58), it immediately follows that

$$v_x(x, y, t, \Phi_1) = -\mathscr{R}e\left[\frac{(a_2{}^2 - 2k_1{}^2)}{k_1 \pi i R(k_1)} \frac{\partial k_1}{\partial t}\right] \chi_1(t, x, y) \tag{68}$$

where χ_1 and k_1 are given by (58) upon substituting y for z. Also,

$$\tilde{v}_y{}^L(k, y, p, \Phi_1) = -\frac{\eta_1(k)(a_2{}^2 - 2k^2)}{R(k)(pk - \xi)} e^{-p\eta_1(k)y},$$

which yields, via equation (58),

$$v_y(x, y, t, \Phi_1) = c_2{}^2 a_1 \delta(t - a_1 y) - \mathscr{R}e\left[\frac{\eta_1(k_1)(a_2{}^2 - 2k_1{}^2)}{\pi i R(k_1) k_1} \frac{\partial k_1}{\partial t}\right] \chi_1(t, x, y). \tag{69}$$

Likewise

$$\tilde{v}_x{}^L(k, y, p, \psi_1) = \frac{2k\eta_1(k)\eta_2(k)}{R(k)(pk - \xi)} e^{-p\eta_2(k)y}.$$

$$\tilde{v}_y{}^L(k, y, p, \psi_1) = -\frac{2k^2\eta_1(k)}{R(k)(pk - \xi)} e^{-p\eta_2(k)y}.$$

These expressions are of the form (59) and automatically yield the results

$$v_x(x, y, t, \psi_1) = \mathscr{R}e \sum_{l=2,3} \frac{2\eta_1(k_l)\eta_2(k_l)}{\pi i R(k_l),} \frac{\partial k_l}{\partial t} \chi_l, \tag{70}$$

$$v_y(x, y, t, \psi_1) = -\mathscr{R}e \sum_{l=2,3} \frac{2k_l\eta_1(k_l)}{\pi i R(k_l)} \frac{\partial k_l}{\partial t} \chi_l, \tag{71}$$

where k_l and χ_l are given by equations (60), with z replaced by y. Equations (68–71) represent the exact solution up to $t = a_1 h$, at which time the terms from $n = 2$ begin to contribute. From equation (44),

$$\tilde{\Phi}^L(k, y, p)_2 = \frac{\tilde{g}^L(k, p)}{p^2 R(k)} (a_2{}^2 - 2k^2)\{[M(k) - 1]XY - M(k)X^2\}e^{p\eta_1(k)y}.$$

This leads to

$$\tilde{v}_x{}^L(k, y, p, \Phi_2) = -\frac{k(a_2{}^2 - 2k^2)}{R(k)(pk - \xi)}\{[M(k) - 1]\exp[-p\eta_2(k)h - p\eta_1(k)(h - y)] - M(k)\exp[-p\eta_1(k)(2h - y)]\}.$$

The first term of the curly brackets is of the same form as equation (61), with $w = h - y$ and $z = h$, while the second term is of the same form as equation (55), with $z = 2h - y$. One can thus write the solution

$$v_x(x, y, t, \Phi_2) = \mathscr{R}e\left\{-\frac{(a_2{}^2 - 2k_4{}^2)[M(k_4) - 1]}{\pi i R(k_4)} \cdot \frac{\partial k_4}{\partial t}\right\}\chi_4(t, x, h, h - y) + \mathscr{R}e\left[\frac{(a_2{}^2 - 2k_1{}^2)M(k_1)}{\pi i R(k_1)} \frac{\partial k_1}{\partial t}\right]\chi_1(t, x, 2h - y), \tag{72}$$

with k_4 and k_1 satisfying $t = \eta_2(k_4)h + \eta_1(k_4)(h - y) + k_4 x$ and $t = \eta_1(k_1)(2h - y) + k_1 x$. The inversion for other values of n proceeds in the same fashion.

Numerical results

To complement the preceding theoretical development, the response to a step time input will now be determined from equations (51–72). In this case, boundary condition (5) reduces to $\tau_{yy}(x, 0, t) = -\mu H(t)H(x)$. This response is given by

$$v(x, y, t) = \int_0^t v(x, y, \tau)_\delta H(t - \tau)\, d\tau,$$

where v stands for either v_x or v_y, and the subscript δ identifies the solution to an impulsive loading; that is $v(x, y, \tau)_\delta$ is the expression contained in (51–72). For the numerical calculation it is more convenient to use the identities

$$\frac{\partial k_n}{\partial t} = \frac{i\eta_n(k_n)}{(t^2 - a_n{}^2\rho^2)^{1/2}}, \quad n = 1, 2, \quad \frac{\partial k_3}{\partial t} = \frac{\eta_2(k_3)}{(a_2{}^2\rho^2 - t^2)^{1/2}}.$$

For k_4 one uses equation (65) to find

$$\frac{\partial k_4}{\partial t} = \eta_1(k)\eta_2(k)[x\eta_1(k)\eta_2(k) - k\eta_2(k)w - k\eta_1(k)z]^{-1},$$

where k on the right side is set equal to k_4. By the form of $\partial k_i/\partial t$, $i = 1, 2, 3$ and equation (B.5), one realizes that these quantities introduce singularities at arrival times. However, these singularities are integrable.

The actual integration was performed using a Legendre–Gauss algorithm in a CDC-6600 computer. The final plot is given for the point $x = 0{\cdot}5h$, $y = 0{\cdot}5h$ and Poisson ratio of 0·25. In Fig. 4 the dimensionless time $T = tc_1/h$ and the dimensionless velocity v_y/c_1 are used. The

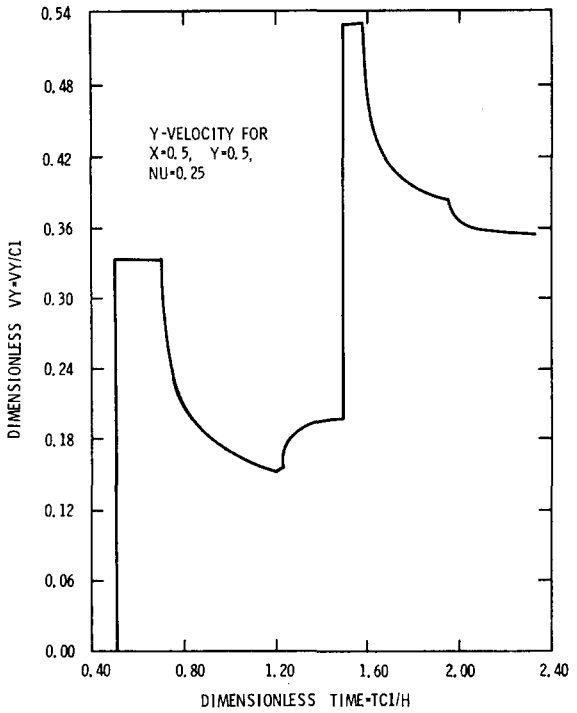

Fig. 4. Y Velocity for $x = y = 0{\cdot}5h$, and Poisson ratio = 0·25.

dimensionless arrival times of the first eight waves are $T = 0{\cdot}500$, 0·707, 1·21, 1·22, 1·50, 1·58, 1·96, 2·34. The first wave is a plane wave below the load; the second, a cylindrical dilatational wave emanating from the point $x = y = 0$; the third, a head wave; the fourth, a cylindrical shear wave also emanating from the point $x = y = 0$; and the fifth, sixth, and seventh, reflected waves.

In Fig. 4, one sees the jump in the y-velocity at the first wave arrival. The second wave is a release wave which reduces the y-velocity induced by the first wave. Another jump occurs at the arrival of the fifth wave, which is a reflected plane wave. In each case, the value of the jump is 1/3. These graphical results are typical of results found at other points sampled in the neighborhood of $y = 0{\cdot}5h$. The x-velocity has no jumps and is zero up to the arrival of the second wave.

DISCUSSION

In the present paper, impact on an elastic plate was considered. An analytical solution was derived by the usual application of integral transforms. Then, using reflection coefficients, ray theory was used to derive another analytical solution. By matrix theory and the use of the interactive program Reduce 2, these solutions were shown to be equivalent. The form of the transform of the solution, as obtained here, made it obvious that there were only three types of integrals for the transform inversion. Thus, in the numerical evaluation for the first five waves, one only needed to change the definition of $F_i(k)$, $i = 1, 2, 3$, to find the x or y velocity. In fact, the program used to evaluate the y velocity was used to evaluate the x velocity by changing a few computer cards, deleting the plane waves, and relabelling the

output. The most important result, however, is that the two dimensional results presented here are readily applicable to the three dimensional case to follow, just as was the case in [6].

Following the results of [6], the solution for a uniform load acting on the strip of finite width: $y = 0$, $-a < x < a$, is then given by

$$^{s}v_j(x, y, t) = v_j(x + a, y, t) - v_j(x - a, y, t),$$

where the superscript s identifies the solution for the strip, and $v_j(x, y, t)$ is the solution for the uniform load acting on $y = 0$, $0 < x < \infty$.

Абстракт — В предлагаемой работе используется недавно разработанный метод, в целью получения решений для упругой пластины под влиянием нагрузок с конечными характеристическими размерностями. Определяются точные двухмерные преобразованные решения для пластинки, внезапно нагруженной по одной из ее ограничающих поверхностей. Для общей нагрузки преобразованное решение располагается еще раз в бесконечные суммы, которые представляют собой многократно отраженные волны сдвига и продольные волны. Интерпретация бесконечных сумм проверена построением хода лучей. Применяются остаточные выражения для вывода функции Грина для скорости. Даются численные результаты для ввода ступенчатой функции.

REFERENCES

1. V. R. Thiruvenkatachar, Stress-Wave Propagation Induced in an Infinite Slab by an Impulse over a Circular Area of one Face—I, *Proc. Nat. Inst. Sci. of India*, Series A, **26**, 31–47 (1960).
2. L. W. Oline, Propagation of the Transverse Normal Stress in a Thick Plate due to Distributed Lateral Impulsive Loadings, Report NASA-TM-X-2568 (September 1972).
3. G. Eason, The Displacements Produced in an Elastic Half-Space by a Suddenly Applied Surface Force, *J. Inst. Maths. and its Applications* **2**, 299–326 (1966).
4. M. Mitra, Disturbance Produced in an Elastic Half-Space by Impulsive Normal Pressure, *Procs. Cambridge Philosophical Society* **60**, 683–696 (1964).
5. M. C. Gutzwiller, The Impact of a Rigid Circular Cylinder on an Elastic Solid, *Phil. Trans. Royal Society of London*, Series A, **255**, 153–191 (1962).
6. F. R. Norwood, Exact Transient Response of an Elastic Half Space Loaded Over a Rectangular Region of its Surface, *J. appl. Mech.* **36**, 516–522 (1969).
7. F. R. Norwood, Interior Motion of an Elastic Half-Space due to a Normal Finite Moving Line Load on its Surface, *Int. J. Solids Struct.* **6**, 1483–1498 (1970).
8. F. R. Norwood, Response of an Elastic Half Space to Impulsive Stationary Finite Line Sources, *J. appl. Mech.* **38**, 549–550 (1971).
9. R. A. Phinney, Calculation of Elastic Wave Propagation in a Layered Medium, Report AD 684 883, Princeton University.
10. S. Timoshenko and J. N. Goodier, *Theory of Elasticity*. McGraw-Hill, New York (1951).
11. H. S. Carslaw and J. C. Jaeger, *Operational Methods in Applied Mathematics*. Oxford University Press (1941).
12. B. van Der Pol and H. Bremmer, *Operational Calculus Based on the Two-Sided Laplace Integral*. Cambridge University Press, London (1964).
13. R. V. Churchill, *Operational Mathematics*, second edition. McGraw-Hill, New York (1958).
14. C. L. Pekeris and I. M. Longman, Ray-Theory Solution of the Problem of Propagation of Explosive Sound in a Layered Liquid, *J. Acoustical Society of America* **30**, 323–328 (1958).
15. L. Knopoff, Surface Motions of a Thick Plate, *J. appl. Phys.* **29**, 661–670 (1958).
16. C. L. Pekeris, Theory of Propagation of Explosive Sound in Shallow Water, Geological Society of America Memoir 27 (1948).
17. C. L. Pekeris, Z. Alterman, F. Abramovici and H. Jarosh, Propagation of a Compressional Pulse in a Layered Solid, *Rev. Geophysics* **3**, 25–47 (1965).
18. C. L. Pekeris, I. M. Longman and H. Lifson, Application of Ray Theory to the Problem of Long-Range Propagation of Explosive Sound in a Layered Liquid, *Bull. Seismological Society of America* **49**, 247–250 (1959).
19. C. L. Pekeris, Z. Alterman and F. Abramovici, Propagation of an SH-Torque in a Layered Solid, *Bull. Seismological Society of America* **53**, 39–57 (1963).
20. L. Knopoff, F. Gilbert and W. L. Pilant, Wave Propagation in a Medium with a Single Layer, *J. Geophysical Research* **65**, 265–278 (1960).

21. A. G. Mencher, Epicentral Displacement Caused by Elastic Waves in an Infinite Slab, *J. Appl. Phys.* **24**, 1240–1246 (1953).
22. R. L. Rosenfeld, Analysis of Long Compressional Elastic Waves in Rods and Plates of Arbitrary Cross Section and Elastic Wave Fronts in Plates and Circular Rods, Ph.D. thesis, California Institute of Technology (1962).
23. F. R. Norwood, Similarity Solutions in Plane Elastodynamics, *Int. J. Solids Struct.* **9**, 789–803 (1973).
24. L. Cagniard, *Reflection and Refraction of Progressive Seismic Waves*. McGraw-Hill, New York (1962) translated by Flinn and Dix.
25. Y. C. Fung, *Foundations of Solid Mechanics*. Prentice-Hall, Englewood Cliffs, N. J. (1965).
26. W. M. Ewing, W. S. Jardetzky and F. Press, *Elastic Waves in Layered Media*. McGraw-Hill, New York (1957).
27. A. C. Hearn, Reduce 2, Decus Program Library, University of Utah, (1971).
28. S. K. Godunov and V. S. Ryabenki, *Theory of Difference Schemes—An Introduction*. North-Holland, Amsterdam (1964).
29. R. A. Frazer, W. J. Duncan and A. R. Collar, *Elementary Matrices*. Cambridge (1960).

APPENDIX A

Derivation of a_n

Equations (46 and 47) imply the recursive relations

$$a_{n+1} = \alpha a_n + b_n \tag{A.1}$$

$$b_{n+1} = \beta a_n \tag{A.2}$$

with the initial values $a_1 = 1, b_1 = 0$. It is important to note here that these recursive relations could easily be solved by the theory of difference equations [28, pp. 9–19]. Equivalently, powers of the matrix $\mathcal{M}$, defined by equation (45), could be obtained by writing $\mathcal{M} = k\Lambda k^{-1}$ as per [29, pp. 64–67]. However, the form obtained for powers of $\mathcal{M}$ is not suitable for the required wave expansion. To find explicitly the expressions for a_n and b_n, the algebraic manipulation system REDUCE 2 was used in the PDP-10 version [27]. This gave the following results:

$$a_1 = \binom{0}{0} = (\alpha + \beta)^0$$

$$a_2 = \binom{1}{0}\alpha \qquad (\alpha + \beta)^1$$

$$a_3 = \binom{2}{0}\alpha^2 + \binom{1}{1}\beta$$

$$a_4 = \alpha\left[\binom{3}{0}\alpha^2 + \binom{2}{1}\beta\right] \qquad (\alpha + \beta)^2$$

$$a_5 = \binom{4}{0}\alpha^4 + \binom{3}{1}\alpha^2\beta + \binom{2}{2}\beta^2$$

$$a_{12} = \alpha\left[\binom{11}{0}\alpha^{10} + \binom{10}{1}a^8\beta + \binom{9}{2}\alpha^6\beta^2 + \binom{8}{3}\alpha^4\beta^3 + \binom{7}{4}\alpha^2\beta^4 + \binom{6}{5}\beta^5\right].$$

For simplicity, only the terms for $(\alpha + \beta)^i$, $i = 0, 1, 2$ are indicated here. Terms for higher values of i may be easily identified. These results led to equation (48), which was verified by mathematical induction. When the explicit values of α and β given by (19) were used in the recursive relations (A.1) and (A.2) the result obtained was

$$a_n = \sum_{r=0}^{n-1} \binom{n+r}{n-r-1} (XY)^{n-r-1} D^r, \qquad D = M^2(k)(X - Y)^2.$$

This result was also verified by mathematical induction.

APPENDIX B

Properties of k_4

For the third case, the Cagniard path is given by $Im[\eta_1(k)w + \eta_2(k)z + kx] = 0$, and may be found by solving

$$t(k) = \eta_1(k)w + \eta_2(k)z + kx \tag{B.1}$$

for k, in terms of w, z, x and t, where t is a real parameter. For fixed values of w, z and x, t may be considered as a parameter which generates Path III. By the branch cuts selected, $\eta_1(k)$ is imaginary on the real axis of the k-plane to the right of the point $k = a_1$. Since t is real, this implies that the intercept of the path with the real axis must satisfy $0 < k_{\text{int}} < a_i$, with no branch cut contribution arising in the third case. Thus, the third case is similar to the first case. Equation (B.1) corresponds to equations (5–5) and (I–1) of [24] and therefore one concludes that the values of t on Path III must satisfy the inequality $t \geq a_1 w + a_2 z$.

When equation (B.1) is rationalized one finds that

$$\begin{aligned} &Ak_4^4 - 4Kk_4^3 + 2Pk_4^2 - 4Qk_4 + E = 0, \qquad (B.2)\\ &A = D^2 - 4z^2w^2, \qquad K = txD, \qquad Q = txT\\ &P = DT + 2t^2x^2 + 2z^2w^2(a_1^2 + a_2^2),\\ &E = T^2 - 4z^2w^2a_1^2a_2^2, \qquad D = x^2 + z^2 + w^2\\ &T = t^2 - z^2a_2^2 - a_1^2w^2. \end{aligned}$$

When $w = 0$ (or $z = 0$) equations (B.1 and B.2) reduce to those for determining $k_2(x, z, t)$ [or $k_1(x, w, t)$]. Note that z and w play similar roles in equation (B.1) and that $4KA^{-1}$ represents the sum of the four roots of (B.2). Thus one deduces that the roots of equation (B.2) differ from $k_2(x, z, t)$ and $k_1(x, w, t)$ by terms which vanish when zh vanishes. This limiting behavior is observed in the following approximate roots valid in the vicinity of $zw = 0$: (a) the approximate root

$$\begin{aligned} Ak = txM + i[AM(T - 2zwa_1a_2) - t^2x^2M^2]^{1/2}, \qquad (B.3)\\ M = x^2 + z^2 + w^2 - 2zw \end{aligned}$$

satisfies equation (B.2) with the last term of P replaced by $4z^2w^2a_1a_2$, and (b)

$$Ak = txM + i\{AM[T - zw(a_1^2 + a_2^2)] - t^2x^2M^2\}^{1/2} \tag{B.4}$$

satisfies equation (B.2) with the second term of E replaced by $-z^2w^2(a_1^2 + a_2^2)$. Numerical results indeed verify the arguments given here.

The time t_3 required in equation (64) may be found by the following argument. The Cagniard path corresponds to the path of steepest descent, and, hence, the intercept with the

real axis, denoted by k_s, is the solution of $\partial t/\partial k = 0$, where t is given by (B.1); i.e.†

$$\left.\frac{\partial t}{\partial k}\right)_{k=k_s} = x - wk/\eta_1(k) - zk/\eta_2(k) = 0. \tag{B.5}$$

When the root k_s of $\partial t/\partial k = 0$ is found, then $t_3 = t(k_s)$ is found from (B.1).

† k_s is the saddle point.